X-Ray Emission Spectra from High-Power-Laser–Produced Plasmas*

B. H. Ripin, P. G. Burkhalter, F. C. Young, J. M. McMahon, D. G. Colombant,† S. E. Bodner, R. R. Whitlock, D. J. Nagel, D. J. Johnson, N. K. Winsor, C. M. Dozier, R. D. Bleach, J. A. Stamper, and E. A. McLean
Naval Research Laboratory, Washington, D. C. 20375
(Received 17 March 1975)

Absolute x-ray emission spectra in the range from 1 to 300 keV were measured from CH_2 plasmas produced at the focus of a high-power ($>10^{16}$ W/cm^2) 1.06-μm laser. Experimental spectra are compared with hydrodynamic-model predictions. The good agreement indicates that suprathermal electrons are unimportant in the interaction and that self-generated magnetic fields dominate the thermal transport.

We report here measurements of absolute x-ray continuum emission spectra from 1 to 300 keV emitted by laser-produced plasmas. These spectra are compared with calculations using a two-dimensional hydrodynamic-model computer code. This wide spectral range yields information about possible suprathermal-electron generation[1-6] and plasma thermal transport.[7] There has been considerable speculation recently upon the importance and implications of these phenomena to laser fusion. Careful measurements were performed of the laser-beam characteristics, focal-spot-intensity distribution, and incident and back-reflected laser energies and spectra. These provide initial conditions for the numerical model. The calculated spectra are in good agreement with experiment if all the transport processes are assumed classical[8] (including spontaneous magnetic fields[9]) without the presence of a suprathermal-electron distribution.

The beam from a Nd laser ($\lambda_0 = 1.06$ μm) was focused at normal incidence upon a planar 0.75-mm-thick polyethylene (CH_2) target in an evacuated ($\sim 10^{-4}$ Torr) chamber. The laser pulse length was 21 ± 2 psec (full width, half-energy) and it was spectrally "chirped" through 4 Å by self-phase modulation as measured by an ultrafast ($\simeq 5$ psec) streak camera viewing a 2-m spectrograph. The laser-intensity distribution at focus has been measured over three decades by ablating a thin film of metal from a glass plate using an attenuated beam, and independently by shooting through a pinhole into a calorimeter at full intensity. The consistency of the low- and high-power focal measurements, shown in Fig. 1, indicates that nonlinear optical effects from the laser and focusing lens were negligible in these experiments. The focal-spot diameter at the target surface (in the absence of plasma) with an $f/1.9$ aspheric lens was 12 μm at half-intensity, with half the laser energy contained within 30 μm diam. Thus, the peak irradiance in the focal spot was over 10^{16} W/cm^2 in these experiments. X-ray pinhole photographs of the plasma indicate that x-ray emission was primarily from within the half-energy diameter of the focal spot.

The possible presence of plasma at the target surface 0.2 nsec before the arrival of the main laser pulse was examined by optical interferometry with a 5320-Å probe beam parallel to the target surface. With only one Pockels cell in the laser for isolation, a low-density plasma ($n_e \simeq 2 \times 10^{18}$ cm^{-3}) with a diameter of about 300 μm was present at the target surface. This plasma results from the leakage of rejected laser oscillator pulses with a maximum energy content of 2 mJ on target.[10] With two Pockels cells, the

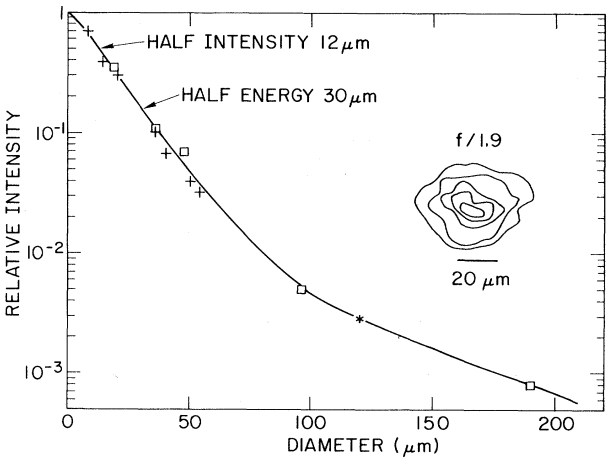

FIG. 1. Focal-spot-intensity distribution. Iso-intensity contours are traced for 3-dB separation. The data for the radial intensity distribution correspond to low-power shots (10^7 W) (+), high-power shots (2×10^{11} W) attenuated before the focusing lens (□), and high-power shot (2×10^{11} W) through a pinhole at the focal position (*).

prepulse energy was measured to be less than 25 μJ and no plasma was detected preceding the laser pulse. No significant change in the x-ray spectra was observed from shots with one or two Pockels cells operating.

The reflection coefficient for laser light scattered from the plasma and returning through the focusing lens was 15% to 20%. Of this approximately 5% was specular reflection and the remainder was interpreted as stimulated Brillouin backscatter.[11] The upper limit of light scattered into all other solid angles was determined to be less than 5% of the incident energy by using calibrated photocopy paper (Hadron, Inc.) wrapped around the target. Thus, between 75% and 80% of the incident laser energy was absorbed by the plasma. This level of energy absorption was found to be insensitive to tilting the target by up to 45° into the plane of polarization.

Thirteen active detectors with x-ray filters were used simultaneously to measure the x-ray spectrum from 1 to 300 keV on each laser shot. Soft x-rays (1 to 6 keV) were measured with silicon p-i-n diodes and x-rays above 6 keV were measured with NaI scintillator-photomultiplier detectors. The scintillation detectors were calibrated absolutely with radioactive sources (^{109}Cd, ^{241}Am, ^{57}Co). p-i-n–diode sensitivity was calculated based on the response of silicon to x rays.[12] Kodak no-screen x-ray film with filters was also employed below 2 keV as a check on intensity. Selected K-edge and broad-band filters were used for energy discrimination as indicated at the top of Fig. 2. The filters were displaced from the scintillators to reduce contributions from fluorescence of the filters. All detectors were located at 135° to the incident-beam direction except the five highest-energy detectors which were located at 45°. Angular isotropy is assumed[13] for x-ray emission below 20 keV in order to normalize 135° to 45° measurements.

A trial x-ray spectrum was used to calculate[14] the signal of each detector using known x-ray attenuation coefficients[15] for the filters and absorption coefficients[15] for the detectors. The shape of the trial spectrum was modified to bring the calculated detector signals into agreement with the measured signals.

Figure 2 presents the envelope of six spectra where the peak laser irradiance in each shot was approximately 1.2×10^{16} W/cm^2. These results corroborate previous measurements[6] in the 5- to 50-keV range when absolute intensities are normalized for the difference in incident laser energies between the two experiments.

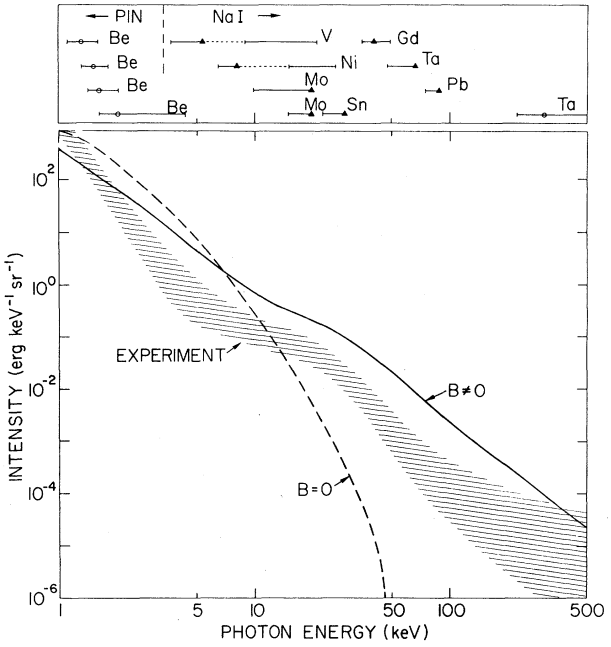

FIG. 2. X-ray intensity versus energy for the experiment and the model calculations. The cross-hatched area spans the range between high and low results observed for six shots. Note the good agreement between experiment and the numerical prediction when magnetic fields are included. The detector ranges (bars) and peak sensitivity energies (points) are indicated across the top of the figure. Broad-band filters are denoted by (○) and K-edge filters by (▲).

It is useful to compare the predictions of a theoretical model with these experimental results in order to understand the x-ray spectra. Free-free x-ray-spectrum diagnostics and a more complete classical thermal-conduction model have been added to an Eulerian two-dimensional hydrodynamic plasma-laser code.[16] This numerical model is distinguished by the use of an equation of state for the plasma and by a complete treatment of thermally self-generated magnetic field effects,[9] including the classical tensor thermal conductivity.[8] Each of these features is important. Thermal-flux limiting has been included without any significant effect indicating that the fluid model is self-consistent. Radiation transport has not been included in the computations because x-ray self-absorption is negligible in the energy range of interest. The initial conditions specified in the code were the laser pulse length, experimental focal-spot-intensity distribution, and a density ramp. It was necessary to assume an initial density ramp for computational

purposes. However the x-ray intensity varied by less than a factor of 3 when the density-gradient scale length was changed by 4 orders of magnitude. The radiation output in each of seventeen frequency intervals is integrated over space and time to obtain the total output.

Calculated x-ray spectra with and without thermally generated magnetic fields are presented along with the experimental results in Fig. 2. The calculation without magnetic fields decreases the high-energy portion of the spectra and is in poor agreement with the experimental spectra above 15 keV. The agreement in shape and magnitude between the spectrum calculated including magnetic fields and the experimental spectra is quite good considering the limitations of the grid size (12 μm) and the uncertainty in assuming emission isotropy. Self-generated magnetic fields with magnitudes comparable to those predicted by the code have been recently directly observed in laser-produced plasmas.[17]

The source of different components of the x-ray spectra may be seen from results of the numerical model such as shown in Fig. 3. The soft-x-ray component (< 3.5 keV) originates in a narrow (~ 12 μm) region inside the critical surface (laser frequency equal to plasma frequency). There, because of the quadratic dependence of the bremsstrahlung power on density, the radiation rate increases even though the temperature is well below its maximum. The harder components (> 3.5 keV) come from hot electrons restrained by the magnetic field near the critical depth. When $\omega_{ce}\tau_e > 1$, heat transport (normal to fields) is reduced from the unmagnetized value by a factor of $\omega_{ce}^2\tau_e^2$. Note that $\omega_{ce}^2\tau_e^2$ reaches a maximum of order 10^6. The peak electron temperature for the $B \neq 0$ case is an order of magnitude higher than for the $B = 0$ case accounting for the harder spectrum when magnetic fields are retained in the calculation. A phenomenon, not included in the calculation, which could account for the decrease of the experimental spectrum above 20 keV is particle drift in an inhomogeneous magnetic field.[18]

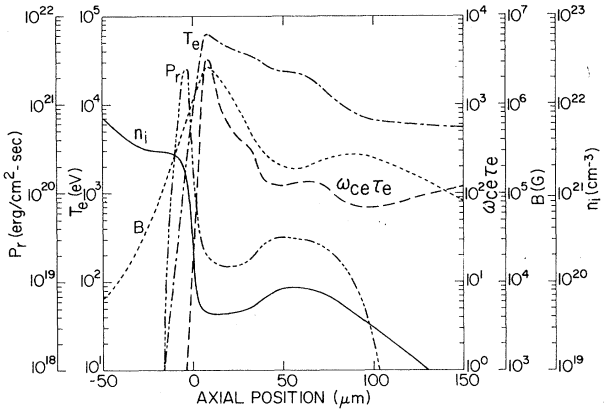

FIG. 3. Calculated axial variations of the magnetic field B, electron temperature T_e, ion density n_i, x-ray production rate P_r, and the dimsionless collision parameter $\omega_{ce}\tau_e$. The electron collision time is τ_e and its cyclotron angular frequency is ω_{ce}. All quantities are computed on axis except for the magnetic field and $\omega_{ce}\tau_e$ which are computed at a radius of 12 μm. The profiles are shown 2 psec after the peak intensity of the laser pulse (1.2×10^{16} W/cm^2). The initial density ramp used in the calculation can be seen from the ends of the mass-density curve.

The agreement between experiment and model calculations performed without assuming suprathermal-electron production strongly suggests that suprathermal electrons are not playing a significant role in this laser-plasma interaction even though the laser irradiance is well above expected parametric-instability thresholds.[1] The addition of suprathermal-electron distributions into the calculations yields x-ray fluences orders of magnitude higher than experiment above 2 keV.[5] To account for the absence of suprathermal electrons we note that parametric decay instabilities require a region several microns thick to absorb a significant fraction of the laser energy. The energy of suprathermal electrons also depends upon the spatial extent of the instability region.[2,18] However, Fig. 3 indicates that the density gradient can be very steep in the absorption region because of the pressure balance of the cold dense plasma with the hot underdense plasma and laser light.[19]

The cause of the excellent absorption observed in this experiment is uncertain. Absorption via decay instabilities is probably negligible because of the steep density gradient. It has been suggested that large plasma electric fields at a rippled critical density surface[20] would heat all electrons by trapping effects rather than by high-phase-velocity waves. Coupling of the laser energy to thermal electrons would also be enhanced if there existed short-wavelength, large-amplitude, ion-density fluctuations.[21] It has also been suggested that the presence of a magnetic field can lead to absorption via slow-phase-velocity waves.

In summary, we have obtained good agreement between experiment and a two-dimensional hydrodynamic model in both the shape and absolute intensity of the emitted x-ray spectra from a laser-

produced plasma. This result has two implications for the laser-fusion program. First, the extent of suprathermal-electron production in such plasmas is very much an open question. Second, we have demonstrated that magnetic fields can dominate thermal transport and must be included in hydrodynamic models. Further research is necessary to determine the reason why the energy absorption is as efficient as found in the experiment.

The many useful discussions with H. D. Shay, R. P. Godwin, and L. S. Levine on the subject of this work were invaluable. The technical assistance of T. DeRieux and E. Turbyfill was appreciated.

*Work supported by the U. S. Energy Research and Development Administration.

†Science Applications, Inc., McLean, Va. 22101.

[1]M. N. Rosenbluth and R. Z. Sagdeev, Comments Plasmas Phys. Contr. Fusion 1, 129 (1972).

[2]J. J. Thompson, R. J. Faehl, W. L. Kruer, and S. Bodner, Phys. Fluids 17, 973 (1974); H. H. Klein and W. M. Manheimer, Phys. Rev. Lett. 33, 953 (1974).

[3]H. Dreicer, R. F. Ellis, and J. C. Ingraham, Phys. Rev. Lett. 31, 426 (1973).

[4]J. Shearer, S. W. Mead, J. Petruzzi, F. Rainer, J. E. Swain, and C. E. Violet, Phys. Rev. A 6, 764 (1972).

[5]V. W. Slivinsky, H. N. Kornblum, and H. D. Shay, to be published.

[6]J. F. Kephart, R. P. Godwin, and G. H. McCall, Appl. Phys. Lett. 25, 108 (1974).

[7]R. P. Godwin, D. V. Giovanielli, and G. H. McCall, Bull. Amer. Phys. Soc. 19, 887 (1974).

[8]S. I. Braginski, in *Reviews of Plasma Physics*, edited by M. A. Leontovich (Consultants Bureau, New York, 1965), Vol. 1, p. 205.

[9]J. A. Stamper, K. Papadopoulos, R. N. Sudan, S. O. Dean, E. A. McLean, and J. M. Dawson, Phys. Rev. Lett. 26, 1012 (1971).

[10]Approximately eight rejected pulses (the most energetic of which is 2 mJ) precede the main pulse at 8-nsec intervals.

[11]B. H. Ripin, J. M. McMahon, E. A. McLean, W. M. Manheimer, and J. A. Stamper, Phys. Rev. Lett. 33, 634 (1974).

[12]J. J. Hohlfelder, in *Advances in X-Ray Analysis*, edited by C. L. Grant *et al.* (Plenum, New York, 1974), Vol. 17, p. 531.

[13]F. C. Young, Phys. Rev. Lett. 33, 747 (1974).

[14]D. H. Johnson, Rev. Sci. Instrum. 45, 191 (1974).

[15]W. H. McMaster, N. Kerr DelGrende, J. H. Mallett, and J. H. Hubbell, University of California Report No. UCRL-50174, Revision 1, 1969 (unpublished).

[16]N. K. Winsor and D. A. Tidman, Phys. Rev. Lett. 31, 1044 (1973).

[17]J. A. Stamper and B. H. Ripin, Phys. Rev. Lett. 34, 138 (1975).

[18]D. A. Tidman and J. A. Stamper, Appl. Phys. Lett. 22, 498 (1973).

[19]Recent experiments tend to corroborate the existence of a steep density gradient at the critical surface. See, for example, K. Eidmann and R. Sigel, Phys. Rev. Lett. 34, 799 (1975); A. Y. Wong and R. L. Stenzel, Phys. Rev. Lett. 34, 727 (1975).

[20]R. A. Shanny, private communication. See also, D. A. Tidman and R. A. Shanny, Phys. Fluids 10, 1207 (1974).

[21]W. L. Kruer, Phys. Fluids 15, 2423 (1972).

Internal Kink Mode in a Diffuse Pinch with a Noncircular Cross Section*

Guy Laval†

Plasma Physics Laboratory, Princeton University, Princeton, New Jersey 08540

(Received 15 July 1974)

It is shown that the internal kink mode is no longer marginally stable within the kink-mode order in a plasma with noncircular cross section. For a step current density with a small ellipticity, the internal kink mode becomes unstable as soon as the rotational transform exceeds 2π close to the magnetic axis.

The internal kink mode in tokamaks has recently received more attention,[1] mainly because of its possible relation with the negative-voltage spikes which are observed in experiments. The $m=1$ internal kink mode occurs whenever the rotational transform exceeds 2π on the magnetic axis. The destabilizing forces are not those which destabilize the usual free-boundary kink modes in the long-wavelength limit. Indeed, if one retains only these effects, the internal kink mode is marginally stable in a circular cross-section discharge.[1] The internal kink mode becomes unstable only if one includes in the stability analysis smaller destabilizing terms which are directly related to the pressure gradient, the magnetic curvature, and finite axial wavelength effects.